



HAL
open science

Three-dimensional Acoustic Radiation Force on an Arbitrary Located Elastic Sphere

Diego Baresch, Jean-Louis Thomas, Régis Marchiano

► **To cite this version:**

Diego Baresch, Jean-Louis Thomas, Régis Marchiano. Three-dimensional Acoustic Radiation Force on an Arbitrary Located Elastic Sphere. Acoustics 2012, Apr 2012, Nantes, France. hal-00810890

HAL Id: hal-00810890

<https://hal.science/hal-00810890>

Submitted on 23 Apr 2012

HAL is a multi-disciplinary open access archive for the deposit and dissemination of scientific research documents, whether they are published or not. The documents may come from teaching and research institutions in France or abroad, or from public or private research centers.

L'archive ouverte pluridisciplinaire **HAL**, est destinée au dépôt et à la diffusion de documents scientifiques de niveau recherche, publiés ou non, émanant des établissements d'enseignement et de recherche français ou étrangers, des laboratoires publics ou privés.



ACOUSTICS 2012

Three-dimensional Acoustic Radiation Force on an Arbitrary Located Elastic Sphere

D. Baresch^a, J.-L. Thomas^a and R. Marchiano^b

^aUPMC-INSP (UMR 7588)/IJLRDA(UMR 7190), 4, Place Jussieu, Cedex 05 - boîte courrier 840, 75252 Paris, France

^bUPMC/CNRS, Institut Jean Le Rond D'Alembert - UMR CNRS 7190, Université Pierre et Marie Curie - 4 place Jussieu, 75005 Paris, France
diego.baresch@upmc.fr

An analytical model for the radiation forces acting on an elastic sphere placed in an arbitrary acoustic wave field is proposed. It provides an expression of the axial and transverse forces without any prescription on the sphere's material, radius or location. To illustrate the capabilities and the generality of the model, we selected a Bessel vortex beam as the incident wave field. Acoustic vortex refers to a type of beam having an helicoidal wavefront. Such a wavefront is due to a screw type phase singularity, hence the beam has a central dark core of zero amplitude surrounded by a high intensity ring. We find that an azimuthal force component appears and is capable of rotating the sphere around the propagation axis. This confirms the transfer of orbital angular momentum from the beam to the sphere. Furthermore, axial forces may turn negative when appropriate parameters are selected and yield a dragging force towards the source of the beam acting as a *Tractor Beam*. In addition to extending the understanding of the nature of acoustic radiation forces, numerical results provide an impetus for further designing acoustic tweezers for potential applications in particle entrapment and non-contact manipulation.

1 Introduction

Non-contact manipulation of particles has many current and potential applications [1]. Pioneer works established the acceleration and entrapment of particles under radiation pressure in light beams [2]. Since then accurate particle manipulations have been demonstrated with "optical tweezers" capable of handling with precision particles ranging from the nanometric to the micrometric scale [3].

Recent research has been concentrated on single-beam particle manipulation in the wave field of a tightly focused transducer [4, 5, 6] and is revealing the ability of ultrasonic beams to accomplish similar tasks. Due to the acoustic nature of the beam, the dimensions of the particles of interest and the corresponding forces increase. Acoustic beams also offer high penetrability in organic tissues and large impedance contrasts with numerous materials. In this manner, "acoustic tweezers" become advantageous and offer extended applications to optical devices.

The precision of optical tweezers comes from complex light interference patterns. In order to trap and then rotate particles, optical vortices were used in early experiments. These light beams are known to carry orbital angular momentum that can be imparted to the particle [7]. Furthermore, the central dark core of this vortex structure provides an entrapment region where the optic or acoustic intensity is minimum. In acoustics, the analogue vortex beams were synthesized with an array of piezoelectric elements in the linear and non-linear regimes [9, 10, 11].

Theoretical investigations of the radiation pressure forces exerted by acoustic beams on spherical particles have only led to the prediction of the axial force when the sphere is on the propagation axis [4, 12]. When the radius of the sphere is much less than the acoustic wavelength, some effort has been made to evaluate the transverse forces for a sphere displaced from the axis of an acoustic vortex [13].

In this paper we present a theoretical model to predict the acoustic radiation forces acting on an elastic sphere in an inviscid fluid. The choice of the beam is *completely arbitrary* and no restrictions are made on the sphere's dimension, material or location. Since the sphere is allowed to be shifted from the beam axis, our model can predict the axial but also the transverse forces both necessary to completely describe the sphere's dynamics under acoustic radiation forces. We apply this analysis to the case of a helicoidal Bessel beam capable of exerting axial, radial and azimuthal forces on an elastic sphere. This analysis should be helpful for potential applications that include particle entrapment and manipulation with single acoustic beams.

2 Method

2.1 Radiation Forces on a sphere in an arbitrary beam

The forces that allow trapping and manipulation of particles in acoustic beams result from the transfer of pseudo linear and sometimes pseudo-angular momentum from the beam to the particle. The particle alters the flux of momentum or angular momentum carried by the beam through scattering. The incident field is supposed to propagate in an inviscid fluid. We neglect effects due to thermo-viscosity and the amplitude of emission is weak enough to discard non-linear effects on the propagation.

To evaluate the radiation pressure, the scattered field has to be determined. The natural choice of coordinate system for the scattering problem is spherical coordinates (r, θ, φ) centered on the sphere (Fig.1). For now, we can write the incident field as the superposition of spherical wave functions Φ_n^m , each of which is solution of the Helmholtz equation in spherical coordinates when the harmonic ($e^{-i\omega t}$) time convention is adopted :

$$(\Delta + k_0^2)\Phi_n^m(r, \theta, \varphi) = 0 \quad (1)$$

The Φ_n^m functions build a natural discrete basis of the problem. Therefore the incident velocity potential ϕ_i can be written [14] :

$$\begin{aligned} \phi_i &= \phi_0 \sum_{n=0}^{\infty} \sum_{m=-n}^n A_n^m \Phi_n^m, \\ \phi_i &= \phi_0 \sum_{n=0}^{\infty} \sum_{m=-n}^n A_n^m j_n(k_0 r) Y_n^m(\theta, \varphi). \end{aligned} \quad (2)$$

Where ϕ_0 is the real amplitude, k_0 is the wavenumber related to the angular frequency and to the phase velocity by $k_0 = \omega/c_0$, $Y_n^m = P_n^m(\cos \theta)e^{im\varphi}$ are complex spherical harmonics (of degree n and order m) and A_n^m are the expansion coefficients for the incident field. The incident wave-field being physically finite at the origin, the radial dependency is described by the spherical Bessel function $j_n(k_0 r)$ and the spherical Neumann functions $y_n(k_0 r)$ are discarded due to their singularity at $r = 0$. The P_n^m functions are the associated Legendre polynomials.

In addition, the scattered velocity potential may be expressed as :

$$\phi_s = \phi_0 \sum_{n=0}^{\infty} \sum_{m=-n}^n A_n^m R_n^m h_n^{(1)}(k_0 r) Y_n^m(\theta, \varphi) \quad (3)$$

Where $h_n^{(1)}(k_0 r) = j_n(k_0 r) + iy_n(k_0 r)$ is the spherical Hankel function of the first kind (that respects Sommerfeld's radi-

ation condition when $r \rightarrow \infty$). As detailed in [15], an arbitrarily shaped beam requires a more general approach to the scattering problem in comparison to the case of an incident plane wave. Anyways, it was proved that the scattering coefficients keep the same expression after applying specific boundary conditions on the surface of the scatterer. We can write :

$$R_n^m \equiv R_n = \alpha_n + i\beta_n \quad (4)$$

R_n are the complex scattering coefficients for each partial spherical wave and are independent from m . These classic coefficients are known for a large variety of spheres under plane wave illumination [16, 17] and only depend on the excitation frequency, the elastic constants of the sphere and the density of the surrounding medium.

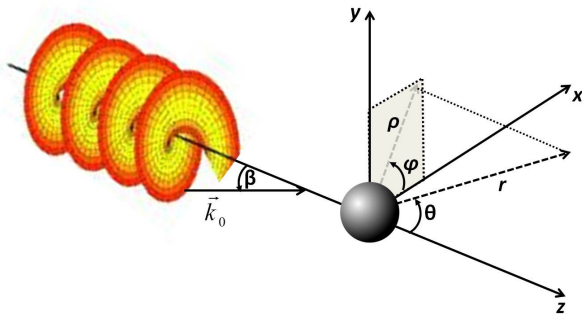


Figure 1: Geometry of the radiation force problem. The sphere is illuminated by an acoustic helicoidal Bessel beam. The reference frame (x, y, z) and the spherical coordinate system (r, θ, φ) are centered on the elastic sphere. The incidence direction of the Bessel beam is described by the half-cone angle β .

The radiation force acting on the particle altering the flux of momentum is obtained by integrating the excess of pressure p over the oscillating surface of the particle $S(t)$. It is defined as an averaged quantity, noted $\langle \cdot \rangle$, over the period $T = 2\pi/\omega$ of the incident field oscillations :

$$\vec{F} = \left\langle \iint_{S(t)} p d\vec{S} \right\rangle \quad (5)$$

Again detailed in [15], some alternatives exist to overcome difficulties owed to integration over a moving boundary. The acoustic pressure p is calculated up to the second order :

$$p = -\rho_0 \frac{\partial \phi}{\partial t} - \rho_0 \frac{(\nabla \phi)^2}{2} + \frac{\rho_0}{2c_0^2} \left(\frac{\partial \phi}{\partial t} \right)^2 \quad (6)$$

Where ϕ is the superposition of the incident and scattered fields [$\phi = (\phi_i + \phi_s)e^{-i\omega t}$]. Rather fastidious calculations that combine Eqs.(2), (3), (4), (5) and (6) lead to the final expression (7) for the three components of the radiation force vector \vec{F} in the Cartesian basis centered on the sphere. \Re and \Im are the real and imaginary parts respectively and $(*)$ designs complex conjugation.

2.2 Incident Beam

We emphasize that the derivation is so far general and expression (7) can be applied to any incident field having

a representation in the spherical basis. However, an important step consists in computing the spherical decomposition of the incident field to obtain the A_n^m coefficients in Eq.(2). They can be obtained numerically using local approximations of the beam in the spherical basis [18]. To minimize numerical errors, it is preferable to use analytical solutions of the decomposition. Several wave fields possess analytical expressions for their decomposition coefficients.

A helicoidal Bessel beam is an example of an acoustic vortex. In cylindrical coordinates (ρ, φ, z) (Fig.1), the spatial part of the complex acoustic velocity potential may be written for a Bessel beam as follows:

$$\phi(\rho, \varphi, z) = \phi_0 J_m(\kappa\rho) e^{i(m\varphi + k_z z)} \quad (8)$$

J_m is the Bessel function of order m . Sometimes referred to the topological charge [8], m is an integer whose sign defines the handedness of the wavefront rotation and its magnitude determines the pitch of the helix. κ and k_z are the radial and axial wave numbers respectively, related by the usual dispersion relation $\kappa^2 + k_z^2 = (\omega/c_0)^2$. An exact expression of a Bessel beam in the spherical basis centered on the sphere exists [19] :

$$A_n^m = i^{n-m} (2n+1) \frac{(n-m)!}{(n+m)!} P_n^m(\cos\beta) \quad (9)$$

Where in this case $\beta = \arcsin(\kappa/k_0)$ has the geometric interpretation of a conic angle (between the wavevector \vec{k}_0 and the propagation axis in Fig.1) in which the Bessel beam is expanded in terms of partial plane waves [20]. On Fig.2 we represented the Bessel beam intensity profile in the (x, y) and (y, z) planes. They are obtained from the summation in Eq.(2) numerically truncated up to $N_{max} = 40$. As can be seen, this beam has a multi-ringed intensity profile that arises from the radial variation of the Bessel function $J_m(\kappa\rho)$. As for any separated variable solution of the Helmholtz equation, the beam is invariant along the propagation axis O_z .

When the sphere is located on the beam axis, the transverse forces F_x and F_y vanish by symmetry. To study radial and sometimes azimuthal forces, the sphere must be displaced off the beam axis. In that case, there is no longer analytical expressions for the expansion coefficients A_n^m . Fortunately, the analytical transformation of spherical wave functions are known under translation or rotation of the initial coordinate system [21, 22]. Thus, from the decomposition of the beam in the initial basis it is possible to calculate the new coefficients A_n^m in a rotated or translated basis centered on the sphere. That is equivalent to displacing the sphere.

3 Results and Discussions

We will now present some numerical results for the radiation force calculation. The procedure is as follows : first we calculate the scattering coefficients R_n for a given sphere. They are known for a large variety of materials and depend of the radius of the sphere a , density ρ' , longitudinal wave speed c_L and transverse wave speed c_T . Then Eq.(7) is applied for different positions of the sphere to obtain the radial, azimuthal and axial forces calculated in a cylindrical reference frame (F_ρ, F_φ, F_z) . We have paid attention in using numerical values corresponding to typical experimental cases, the incident medium is taken to be water having a density $\rho_0 = 1000\text{kg/m}^3$ and the speed of sound is $c_0 = 1500\text{m/s}$.

$$\begin{aligned}
F_x &= -\frac{\pi\rho_0\phi_0^2}{2} \sum_{n=0}^{\infty} \sum_{|m|<n} Q_n^m \left[(V_n^m \Im\{A_n^m A_{n+1}^{m+1*}\} - \Im\{A_n^m A_{n+1}^{m-1*}\}) D_n^1 - (V_n^m \Re\{A_n^m A_{n+1}^{m+1*}\} - \Re\{A_n^m A_{n+1}^{m-1*}\}) D_n^2 \right] \\
F_y &= -\frac{\pi\rho_0\phi_0^2}{2} \sum_{n=0}^{\infty} \sum_{|m|<n} Q_n^m \left[-(V_n^m \Re\{A_n^m A_{n+1}^{m+1*}\} + \Re\{A_n^m A_{n+1}^{m-1*}\}) D_n^1 - (V_n^m \Im\{A_n^m A_{n+1}^{m+1*}\} + \Im\{A_n^m A_{n+1}^{m-1*}\}) D_n^2 \right] \\
F_z &= -\frac{\pi\rho_0\phi_0^2}{2} \sum_{n=0}^{\infty} \sum_{|m|<n} 2(n+m+1) Q_n^m \left[\Re\{A_n^m A_{n+1}^{m*}\} D_n^2 - \Im\{A_n^m A_{n+1}^{m*}\} D_n^1 \right]
\end{aligned} \tag{7}$$

$$\text{where } D_n^1 = \alpha_n + \alpha_{n+1} + 2(\alpha_n \alpha_{n+1} + \beta_n \beta_{n+1}) \quad , \quad D_n^2 = \beta_{n+1} - \beta_n + 2(\beta_{n+1} \alpha_n - \alpha_{n+1} \beta_n)$$

$$\text{And } Q_n^m = \frac{2(n+m)!}{(2n+1)(2n+3)(n-m)!} \quad , \quad V_n^m = (n+m+1)(n+m+2)$$

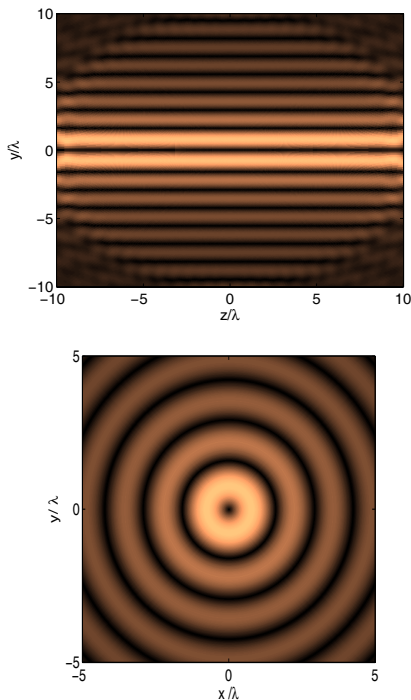


Figure 2: Intensity profiles of the incident Bessel Beam in the (y, z) and (x, y) planes. Lengths are in units of the acoustic wavelength λ

The incident wave has a pressure amplitude $P_0 = 0.1$ MPa and the driving frequency is $f = 1$ MHz. Under these conditions, the wavelength is $\lambda = 1.5$ mm.

3.1 Axial force on spheres in a Bessel Beam

First we will present examples of the axial force calculation F_z . The incident wave field is a Bessel beam having a half-cone angle $\beta = 40^\circ$ and a topological charge $m = 1$. In Fig.3 we show the axial force as a function of the dimensionless radius a/λ of two different spheres. It is clear from the comparison with a rigid sphere (typically the case of aluminum) that when elasticity is taken into account (nylon case) the force exhibits intense peaks. Those resonances in the a dependency of the scattering coefficients R_n are associated to weakly damped waves guided by the surface of the sphere [12]. The resonance peaks are strongly dependent on the topological charge m and the half-cone angle β (data not shown).

In Fig.4, for three different values of the half-cone angle β we depict the axial force F_z for a polystyrene sphere as a

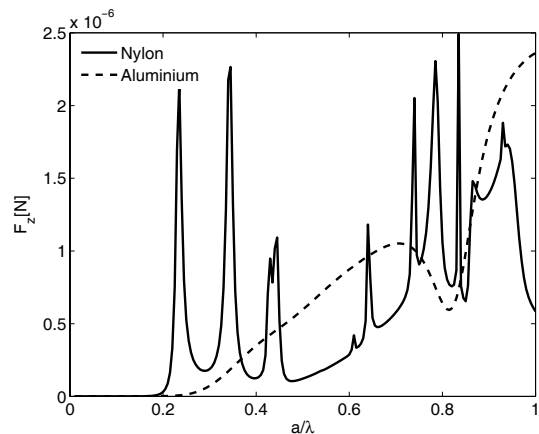


Figure 3: Axial force (Newtons) exerted by a Bessel beam with topological charge $m = 1$ on Nylon and Aluminium spheres as a function of the dimensionless radius a .

function of its radius, a . It shows that for $\beta = 60^\circ$ and 70° there is a region for a where $F_z < 0$: $0.34\lambda \leq a \leq 0.39\lambda$ and $0.28\lambda \leq a \leq 0.32\lambda$ respectively. That means that the force is directed towards the source of the beam. In [12] similar calculations had predicted this unexpected negative axial radiation force for elastic, rigid and liquid spheres on the axis of Bessel beams. Nevertheless, the potential application that consists in using Bessel beams as *Tractor beams* relies on both negative axial forces and the transverse stability of the sphere that is still unexplored.

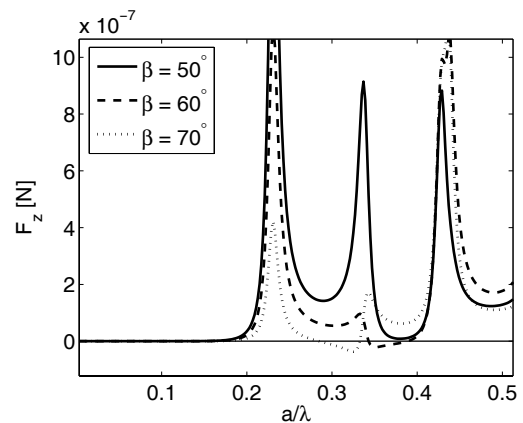


Figure 4: Axial force (Newtons) exerted by a Bessel beam with topological charge $m = 1$ on a polystyrene sphere as a function of the dimensionless radius a . Three different values of the parameter β are selected.

3.2 Transverse forces on a sphere

Figure 5 shows the radial force F_ρ as a function of the distance of displacement ρ for selected parameters that correspond to the negative extrema in the dashed and dotted curves in Fig.4 : $(a, \beta) = (0.35\lambda, 60^\circ)$ and $(a, \beta) = (0.32\lambda, 70^\circ)$. A radial equilibrium position is obtained when both $F_\rho(\rho) = 0$ and the slope is negative since for any displacement of the sphere an opposite force appears. For $\beta = 70^\circ$, we see that the sphere is not trapped in the core of the vortex so it will not be dragged up the propagation axis. The only equilibrium position in this case is located at a distance $\rho = 0.48\lambda$. Contrarily, for $\beta = 60^\circ$, we see that the sphere can be trapped and maintained in the central core, meanwhile it is dragged towards the source because of the negative axial force ($F_z = -21.5$ nN).

Figure 6 shows that an azimuthal force also appears in the transverse plane. The sphere will start spinning around the beam axis due to the azimuthal forces. This confirms the transfer of pseudo-angular momentum from the beam to the sphere.

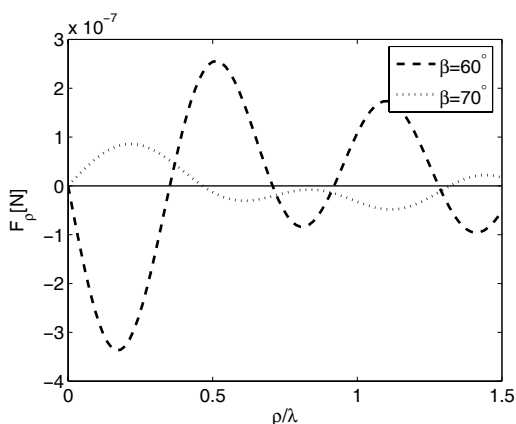


Figure 5: Radial force (Newtons) exerted by a Bessel beam with topological charge $m = 1$ on a polystyrene sphere with parameters $\beta = 60^\circ$ and $a = 0.35\lambda$ (dashed curve). The dotted curve is for $\beta = 70^\circ$ and $a = 0.32\lambda$. Both cases correspond to the negative extrema in Fig.4.

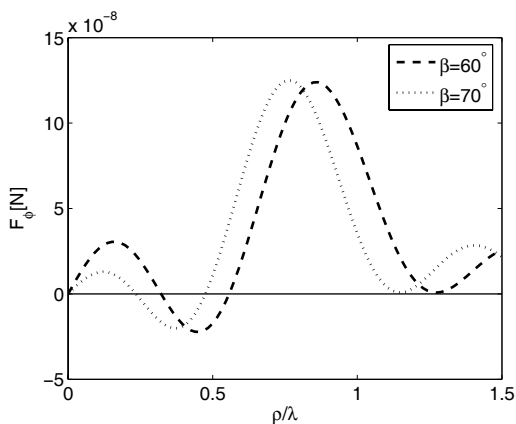


Figure 6: Azimuthal force (Newtons) same sphere and beam parameters than in Fig.5.

As expected, the transverse behavior will also depend on the sphere's material. In that matter, for a radius $a = 0.3\lambda$ and a beam parameter $\beta = 40^\circ$, a polystyrene sphere will be urged away from the beam core (Fig.7) meanwhile the

aluminum sphere will strongly be attracted towards the propagation axis (Fig.8). This is in agreement with King's initial work on radiation forces on spheres in a standing plane waves [23]. He had predicted that light spheres (in comparison to the density of the propagation medium) were attracted to pressure anti-nodes and dense spheres to pressure nodes. In fact, the Bessel beam intensity profile (Fig.2) can be understood to have a collection of nodes and anti-nodes in the radial direction.

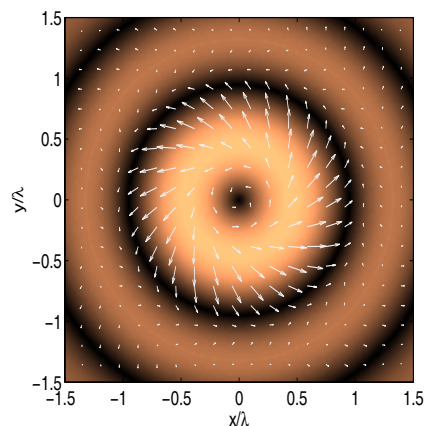


Figure 7: Transverse stability of a polystyrene sphere (with $a = 0.3\lambda$) in the field of a Bessel beam with topological charge $m = 1$. The 2D grey-scale represents the beam's intensity profile.

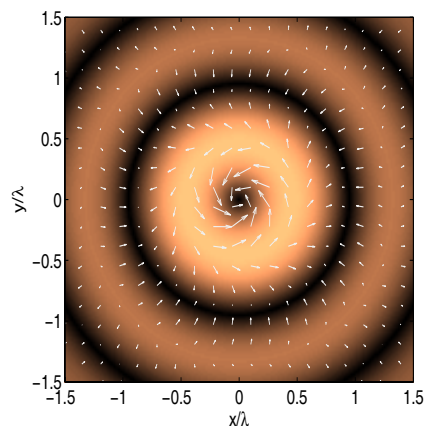


Figure 8: Transverse stability of an aluminum sphere (with $a = 0.3\lambda$) in the field of a Bessel beam with topological charge $m = 1$.

4 Conclusion

In this work, we derived an expression for the three dimensional radiation force on a sphere in an inviscid fluid. To our knowledge, for the first time in acoustics it is possible to analyze the axial and transverse stability of an arbitrarily located sphere. There is no restrictions on the sphere's dimension or material. Eq.(7) is sufficiently general and can be applied to any incident wave field that can be expanded in the spherical basis centered on the sphere. We remind that all complications owed to thermo-viscosity were neglected

in this work and consequent errors may arise when the radius of the sphere is not much larger than the thickness of the thermal-viscous boundary layer [24]. However, for many potential applications these effects are negligible.

In order to illustrate our model, we concentrated our efforts on calculating the trapping efficiency of incident helicoidal Bessel beams. It was shown that important peaks in the axial force arise when an elastic nylon sphere was considered. As it was initially observed in [12], for specific high values of the β parameter a surprising reversal of the axial force may lead to beams that can pull the sphere towards the acoustic source. Here we proved that situations with negative F_z are not systematically associated to a radial attracting force towards the propagation axis. This last condition is required in order to investigate the potential use of a Bessel beam as a *tractor beam*. The spheres can rotate around the beam axis due to the transfer of orbital angular momentum through scattering by a the sphere off-axis.

We proposed a general model that should be helpful to elaborate acoustic devices for non-contact manipulation of small objects. "Acoustic tweezers" have promising applications in small particle entrapment and manipulation including *in vivo* applications.

References

- [1] A. Ashkin, "History of optical trapping and manipulation of small-neutral particle, atoms, and molecules", *IEEE Quant. Elec.* **6**, 841–856 (2000).
- [2] A. Ashkin, "Acceleration and trapping of particles by radiation pressure", *Phys. Rev. Lett.* **24**, 156 (1970).
- [3] D.G. Grier, "A revolution in optical manipulation", *Nature* **424**, 810–816 (2003).
- [4] X. Chen and R. Apfel, "Radiation force on a spherical object in the field of a focused cylindrical transducer", *J. Acoust. Soc. Am.* **101**, 2443–2447 (1996).
- [5] J. Lee, S. Teh, A. Lee, H. H. Kim, C. Lee, and K. K. Shung, "Single beam acoustic trapping", *App. Phys. Lett.* **95**, 1–3 (2009).
- [6] J. Lee and K. Shung, "Radiation forces exerted on arbitrarily located sphere by acoustic tweezer", *J. Acoust. Soc. Am.* **120**, 1084–1094 (2006).
- [7] M. Padgett, S. Barnett, and R. Loudon, "The angular momentum of light inside a dielectric", *J. Mod. Opt* **50**, 1555–1562 (2003).
- [8] J.-L. Thomas, T. Brunet, and F. Coulouvrat, "Generalization of helicoidal beams for short pulses", *Phys. Rev. E.* **81**, 1–14 (2010).
- [9] J.-L. Thomas and R. Marchiano, "Pseudo angular momentum and topological charge conservation for nonlinear acoustical vortices", *Phys. Rev. Lett.* **91**, 1–4 (2003).
- [10] J.-L. Thomas and R. Marchiano, "Synthesis and analysis of linear and nonlinear acoustical vortices", *Phys. Rev. E.* **71**, 1–11 (2005).
- [11] R. Marchiano and J.-L. Thomas, "Doing arithmetic with nonlinear acoustic vortices", *Phys. Rev. L.* **101**, 1–4 (2008).
- [12] P. Marston, "Radiation force of a helicoidal Bessel beam on a sphere", *J. Acoust. Soc. Am.* **120**, 3539–3547 (2009).
- [13] S. Kang and C. Yeh, "Potential-well model in acoustic tweezers", *IEEE Ultrasonics* **57**, 1451–1459 (2010).
- [14] D. Blackstock, *Fundamentals of physical acoustics*, chapter 10 (John Wiley & Sons, New York) (2000).
- [15] D. Baresch, J.-L. Thomas, and R. Marchiano, "Three-dimensional acoustic radiation force on an arbitrarily located elastic sphere", *J. Acoust. Soc. Am.* (Submitted December 2012).
- [16] J. Faran, "Sound scattering by solid cylinders and spheres", *J. Acoust. Soc. Am.* **23**, 405–418 (1951).
- [17] P. Epstein and R. Carhart, "The absorption of sound in suspensions and emulsions. i. water fog in air.", *J. Acoust. Soc. Am.* **25**, 553–565 (1953).
- [18] G. Gouesbet, J. Lock, and G. Grehan, "Generalized Lorenz Mie theories and description of electromagnetic arbitrary shaped beams : Localized approximations and localized beam models, a review", *J. Quant. Spect. and Rad. Transf.* **112**, 1–27 (2010).
- [19] J. Stratton, *Electromagnetic Theory*, chapter 6-7 (McGraw-Hill, New York) (1941).
- [20] P. Marston, "Scattering of a Bessel beam by a sphere: II. helicoidal case and spherical shell example", *J. Acoust. Soc. Am.* **124**, 2905–2910 (2008).
- [21] G. Videen, *Light Scattering from Microstructures*, 81–96 (Springer, Berlin) (2000).
- [22] C. H. Choi, C. C. J. Ivancic, M. Gordon, and K. Ruedenberg, "Rapid and stable determination of rotation matrices between spherical harmonics by direct recursion", *J. Chem. Phys.* **111**, 8825–8831 (1987).
- [23] L. King, "On the acoustic radiation pressure on spheres", *Proc. R. Soc. London* **147**, 212–214 (1935).
- [24] S. Danilov and M. Mironov, "Mean force on a small sphere in a sound field in a viscous fluid", *J. Acoust. Soc. Am.* **107**, 143–153 (2000).